Pressure-induced symmetry breaking in tetragonal $CsAuI_3$

Shibing Wang,[1,2] Shigeto Hirai,[1] Max C. Shapiro,[3] Scott C. Riggs,[3] Ted H. Geballe,[3] Wendy L. Mao,[1,4] and Ian R. Fisher[3]
[1]*Department of Geological and Environmental Sciences, Stanford University, Stanford, California 94305, USA*
[2]*SSRL, SLAC National Accelerator Laboratory, Menlo Park, California 94025, USA*
[3]*Department of Applied Physics, Geballe Laboratory for Advanced Materials, Stanford University, Stanford, California 94305, USA*
[4]*Photon Science, SLAC National Accelerator Laboratory, Menlo Park, California 94025, USA*
(Received 4 May 2012; revised manuscript received 24 October 2012; published 6 February 2013)

Results of *in situ* high-pressure x-ray powder diffraction on the mixed-valence compound $Cs_2Au^{I}Au^{III}I_6$ ($CsAuI_3$) are reported for pressures up to 21 GPa in a diamond-anvil cell under hydrostatic conditions. We find a reversible pressure-induced tetragonal-to-orthorhombic structural transition at 5.5–6 GPa and reversible amorphization at 12–14 GPa. Two alternative structures are proposed for the high-pressure orthorhombic phase and are discussed in the context of a possible Au valence transition.

DOI: 10.1103/PhysRevB.87.054104 PACS number(s): 61.05.cp, 62.50.−p, 71.45.Lr

I. INTRODUCTION

As a fundamental thermodynamic parameter, pressure can dramatically alter materials' properties and can induce structural, electronic, and/or magnetic transitions. Among these, pressure-induced valence transitions have attracted wide interest because they provide a platform for studying the interplay between electronic and lattice degrees of freedom and the discovery of emergent behavior. For example, in $4f$ electron systems, such as rare-earth chalcogenides, the valence of the rare-earth ion can be controlled either with applied pressure or by varying the chalcogen.[1] Another interesting group of mixed valence compounds originates from strong electron-phonon coupling in certain $5d$ transition-metal systems. Unlike valence fluctuations in $4f$ materials, they exhibit a mixed-valence ground state with d^{n-1} and d^{n+1} electron configurations.

The family of alkali-metal gold halides $M_2Au_2X_6$ (M = K, Rb, or Cs; X = Cl, Br, or I) is a prototypical example of such "valence-skipping" mixed-valence $5d$ compounds and has attracted considerable attention due to its sensitivity to applied pressure.[2,3] In particular, $CsAuX_3$ (X = Cl, Br, or I) has been widely studied because of its relatively simple tetragonal perovskite structure. Evidence from early experiments indicated that pressure led to a higher crystal symmetry through a first-order structural transition for the chloride, bromide, and iodide at 12.5, 9, and 5.5 GPa, respectively.[4–6] Additional experimental evidence based on Raman spectroscopy[7] and Mössbauer spectroscopy[8,9] suggests that, coupled to the structural transition, there is an associated mixed-valence (MV) to single-valence (SV) transition, although it is not clear whether these necessarily occur at exactly the same pressure and temperature.[6] In order to understand the origin of the suppression of this charge-density wave state with applied pressure, it is necessary to carefully investigate the evolution of the crystal structure, which is the purpose of the current paper.

Among the alkali-metal gold halides, the critical pressure for the structural transition is the lowest for $CsAuI_3$, presumably due to the increased hybridization between Au $5d$ states and I $5p$ states compared with lighter halogens. At ambient conditions, $Au^{I}I_2$ and $Au^{III}I_4$ adopt a linear and square planar configuration, respectively (cf. Fig. 1) and have an alternating arrangement, forming a distorted perovskite structure with tetragonal space group $I4/mmm$.[10,11] The compound undergoes a first-order structural transition at 5.5 GPa. Initial experiments indicated that both I(1) and I(2) iodine ions moved to the midpoint of the two Au cations in the horizontal and vertical directions, respectively, yielding a tetragonal structure with two equivalent Au sites.[5,6,12] The ^{197}Au Mössbauer spectroscopy measurements conducted on $CsAuI_3$ at 4.2 K suggest the fully Au^{II} SV state occurs at much higher pressures between 6.6 and 12.5 GPa.[8] Applied pressure also strongly affects transport properties. With increasing pressure, the resistivity, at first, exhibits a reduction in the band gap and even a metallic temperature dependence, but the eventual structural transition yields semiconducting behavior, previously attributed to a band Jahn-Teller effect associated with the Au^{II} $5d^9$ electronic configuration.[6,12] A more recent paper on the high-pressure structure and transport properties of $CsAuI_3$ found that the metallic state was not observed up to 20 GPa at which pressure the compound became amorphous.[13] Recent pump-probe experiments, measuring the lifetime of the intervalence charge transfer, suggest that photoinduced excitation has a similar effect to hydrostatic pressure and further suggests the nonmetallic nature of the excited Au^{II} state.[14]

The discrepancies in transition pressure and measured conductivity between previous measurements of $CsAuI_3$ may be due to the resolution of the previous experimental measurements and the different pressure-transmitting media chosen. The alkali-metal gold halide family is clearly very sensitive to deviatoric stress: A recent high-pressure paper on the structure of $CsAuCl_3$ using He as the pressure-transmitting medium found a pressure-induced transition to a cubic phase at 12.5 GPa,[4] contradicting the previous reports that either a cubic structure emerges at 5.2 GPa (Ref. 15) or a high-pressure tetragonal phase appears at 11 to 12 GPa.[5]

In this paper, we present a study on the high-pressure structure of $CsAuI_3$ measured in a hydrostatic environment using synchrotron x-ray powder diffraction. In contrast to previous results, we find that hydrostatic pressure breaks the rotational symmetry of the ab plane and a tetragonal-to-orthorhombic phase transition occurs at 5.5–6 GPa. Our results do not permit a unique determination of the orthorhombic structure but do clearly point to two possible solutions. We discuss these in the context of the Au valence transition.

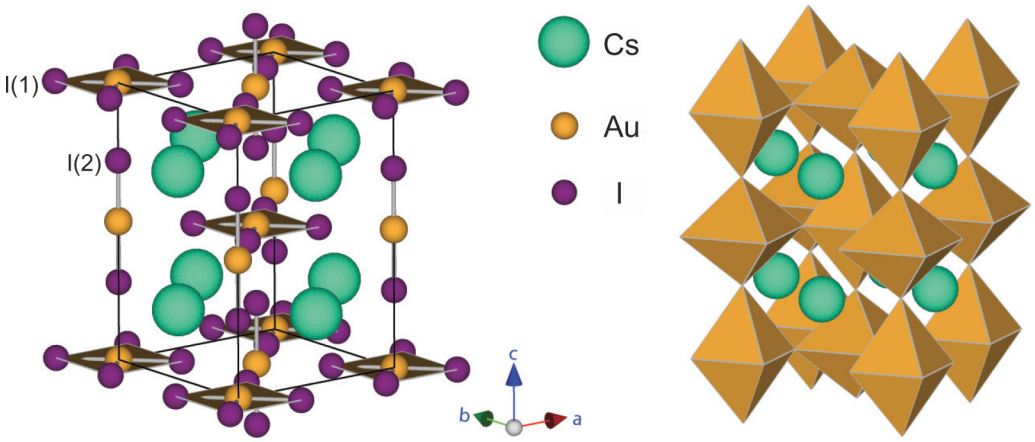

FIG. 1. (Color online) Ambient pressure crystal structure of $CsAuI_3$ at 300 K. The left panel shows the linear and square planar coordinations of $Au^{I}I_2$ and $Au^{III}I_4$, respectively. We denote I^- as I(1) for those associated with square planar $Au^{III}I_4$ and I^- as I(2) for those associated with the linear $Au^{I}I_2$. The right panel shows the structure in alternating elongated and compressed AuI_6 octahedra, more clearly revealing the distorted perovskite structure.

II. EXPERIMENTAL

$CsAuI_3$ crystals were grown by a self-flux method as described elsewhere[16] using CsI, Au, and I_2 as starting materials. The sample was ground into a powder and was loaded into a 150-μm diameter sample chamber drilled into a stainless-steel gasket compressed between two diamonds with a 500-μm culet diameter inside a symmetric diamond-anvil cell (DAC). To maintain hydrostatic conditions, Ne was chosen as the pressure-transmitting medium, which was loaded into the DAC using the gas-loading system at GSECARS of the Advanced Photon Source, Argonne National Laboratory. A small ruby chip placed in the DAC was used for pressure calibration by observing the ruby R1 fluorescence line.[17] Good hydrostaticity was maintained up to the highest pressures measured. *In situ* high-pressure angle-dispersive powder x-ray diffraction (XRD) was conducted at Beamline 12.2.2 of the Advanced Light Source (ALS) at Lawrence Berkeley National Laboratory with an incident x-ray wavelength of 0.4959 Å. Two-dimensional diffraction patterns from the MAR345 image plate were integrated using FIT2D.[18] Rietveld refinement was performed on the powder-diffraction pattern using the GSAS-EXPGUI package.[19]

III. RESULTS AND DISCUSSION

Angle-dispersive XRD was conducted under hydrostatic compression up to 21.2 GPa. Selected spectra during the increasing pressure cycle are shown in Fig. 2. At 5.9 GPa, a new high-pressure phase starts to emerge, coexisting with the original tetragonal phase. The transition pressure is consistent with the previous results of 5.5 GPa,[5,13] but as described below, we have assigned the high-pressure structure to be orthorhombic. The orthorhombic phase persists until 14.2 GPa above which the (112)(200)(020) triplet at $2\theta \approx 7.3^\circ$ is nearly gone and only two groups of broad peaks are present. This observation is consistent with the XRD spectra at similar pressures in the recent paper of Kusmartseva *et al.*[13] where they pointed out the compound starts to become amorphous above 12 GPa. As shown in Fig. 3, during the decompression cycle, crystalline XRD peaks reemerge at 12.5 GPa, indicating the return of the high-pressure crystalline phase. As pressure was further released to 4.5 GPa, the diffraction pattern clearly differed from the orthorhombic phase and resembled the low-pressure tetragonal phase. Although the diffraction pattern at the lowest pressure during the decompression cycle is not as well resolved as those during the compression cycle, we can clearly see that the pressure-induced amorphization of $CsAuI_3$ up to 21 GPa is reversible. This finding contrasts with the previous result that the amorphous phase can be quenched to ambient pressure after being compressed to 32 GPa in a nonhydrostatic environment.[13] Such differences indicate that structural transformation and phase stability in $CsAuI_3$ are very sensitive to the degree of hydrostaticity.

In our XRD spectra (cf. Fig. 4), we see a triplet emerging from the 112 and 200 doublet above 6 GPa that was not reported in previous literature. The absence of this feature in

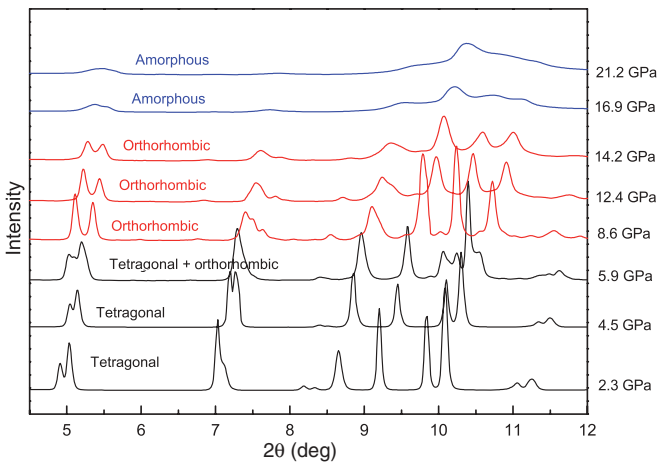

FIG. 2. (Color online) Selected angle-dispersive x-ray powder-diffraction patterns for $CsAuI_3$ at 300 K taken upon increasing pressure. Black curves: tetragonal phase; red curves: orthorhombic phase; and blue curves: amorphous phase. At 5.9 GPa, there is a coexistence of the tetragonal and orthorhombic phases.

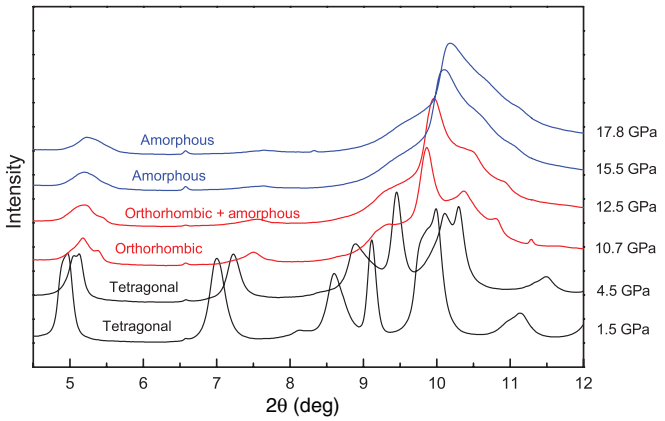

FIG. 3. (Color online) Selected angle-dispersive x-ray powder-diffraction patterns for $CsAuI_3$ at 300 K taken upon the decompression cycle. Black curves: tetragonal phase; red curves: orthorhombic phase; and blue curves: amorphous phase. The patterns indicate that the amorphization is reversible.

earlier experiments is likely due to diffraction peak broadening that can occur under deviatoric stress when less hydrostatic pressure-transmitting media are used. The triplet feature in our spectra is due to the 200 peak splitting into the 200 and 020 reflections in the orthorhombic phase. The asymmetric feature at $2\theta \approx 9^\circ$ indicates the 2θ value of 202 and 022 reflections are no longer equal. The splitting of these Bragg reflections suggests that the high-pressure structure adopts a lower-symmetry space group in which the original rotational symmetry in the *ab* plane is broken. We eliminated the possibility of a monoclinic space group that was isostructural to $RbAuI_3$ because this yielded a higher volume than the original tetragonal phase. We also notice the persistence of the 103 and 211 features at $2\theta \approx 8.5^\circ$ in contrast to previous results that the features are not observable after the structural phase transition.[5,12]

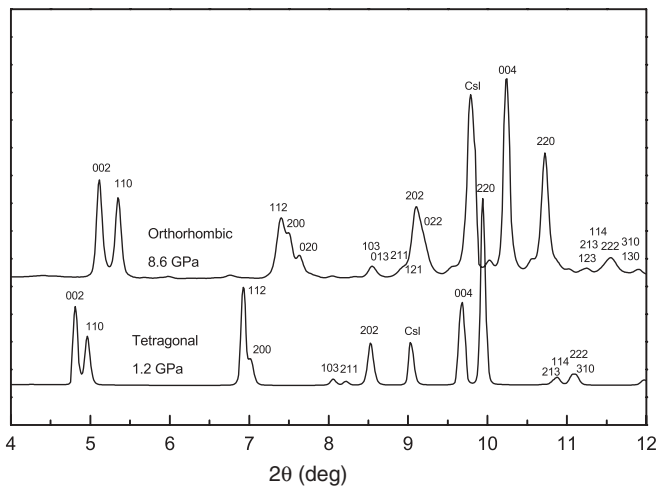

FIG. 4. Indexed XRD patterns for the low-pressure tetragonal phase at 1.2 GPa and high-pressure orthorhombic phase at 8.6 GPa. The 112 and 200 doublet feature in the tetragonal phase evolves to a triplet of 112, 200, and 020 reflections in the orthorhombic phase. The peak marked with CsI is the strongest 110 reflection of simple cubic CsI.

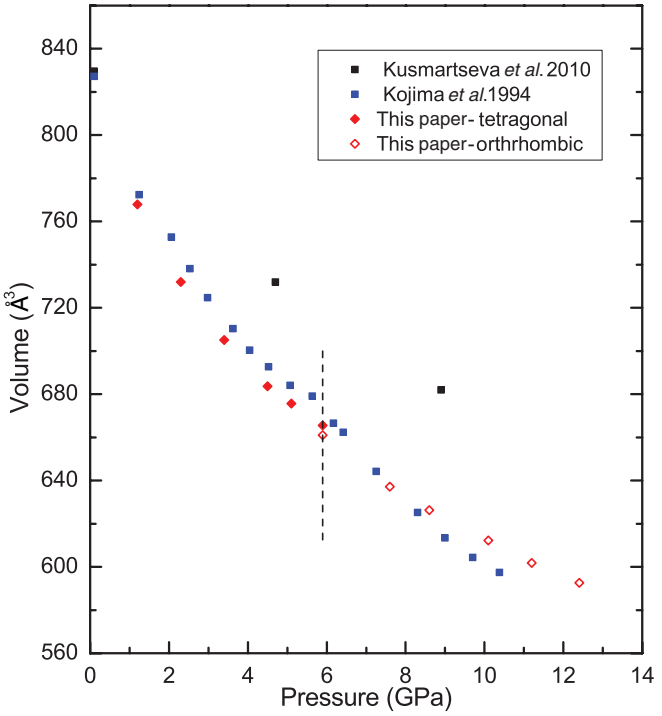

FIG. 5. (Color online) Evolution of the unit-cell volume of $CsAuI_3$ with pressure at 300 K compared with previously published results. Black squares represent data from Ref. 12, and blue squares are from Ref. 5. Red diamonds are from this paper, filled symbols represent the low-pressure tetragonal phase, and unfilled symbols represent the high-pressure orthorhombic phase. The vertical dashed line marks the onset of the first-order pressure-induced phase transition for increasing pressures.

The pressure dependence of the unit-cell volume of $CsAuI_3$ is presented in Fig. 5. At 5.9 GPa, the orthorhombic phase shows a volume reduction of 0.7%. In the lower-pressure tetragonal phase, our measurements give a smaller volume compared to previous results. This could be due to the pressure environment. In the axial diffraction geometry, the Bragg reflections, sampled by the detector, are those whose planes are nearly parallel to the compression axis. In a nonhydrostatic environment, uniaxial compression tends to result in planes perpendicular to the compression axis being more compressed and those parallel to the compression axis being less compressed. Therefore, the larger volume in the paper of Kusmartseva *et al.* may be a result of their lack of use of any pressure-transmitting medium.[13] The slightly different trend in the volume change for the higher-pressure phase above 5.5 GPa is due to the different crystal system assignments.

In previous energy-dispersive and angle-dispersive XRD studies, the high-pressure phase above 5.5–6 GPa was identified as tetragonal with possible space group $P4/mmm$.[5,6,12,13] In this assignment, the I^- ions are located exactly at the midpoint of the two Au ions, making the two Au sites crystallographically equivalent. This result was evidenced by the observation of the weakening and the eventual disappearance of the 103 and 211 reflections as pressure increases to approximately 5 GPa.[5,12] In our paper, however, the persistence of the 103 and 211 reflections in both the tetragonal and

the orthorhombic phases suggests the I^-'s are not in the midpoints between the two Au sites of (0,0,0) and (0,0,1/2). There can be a result of, at least, two types of distortion to this: (i) I(2) deviates from the midpoint but remains in the midplane of the above-mentioned two Au sites, i.e., I(2) is at (δx,δy,1/4); (ii) I(2) stays in line with the two Au sites but deviates from the midpoint, i.e., I(2) is at $(0,0,1/4+\delta z)$. Two space groups, *Ibmm* and *Immm*, that fit the diffraction spectra equally well, correspond to the two scenarios described above. The difference between these two space groups is that certain Bragg reflections that are forbidden in the *Ibmm* space group are allowed in the lower-symmetry *Immm* space group. Among the major Bragg peaks of orthorhombic $CsAuI_3$, at the 103 reflection, *Immm* has an additional 013 reflection with a 2θ value 0.028° higher than that of the 103 reflection. Such features, however, cannot be unambiguously resolved in our spectra due to strain broadening and limited instrument resolution.

With *Ibmm* or *Immm*, we obtained almost the same lattice parameter for the orthorhombic phase. Their pressure dependences are plotted in Fig. 6(a) together with the lattice parameters for the tetragonal $I4/mmm$ low-pressure phase. At the structural phase transition at 5.9 GPa, the length of the c axis increases by 1.6%, whereas, a and b shrink by 0.3% and 2% compared with a in the tetragonal phase. If we further plot the difference in a and b, i.e., the strain of the orthorhombic cell $2(a-b)/(a+b)$ (Ref. 20) with pressure, we see the value nearly doubles from 7.6 to 12.4 GPa (inset of Fig. 6). For the supercell of the perovskite structure (ABX_3), the ratio $c/\sqrt{2}a$ represents the average distortion in the BX_6 octahedra along the c axis. A value of 1.0 usually implies perfect symmetric BX_6 octahedra in the structure. When the structure distorts to an orthorhombic symmetry, we use $c/\sqrt{a^2+b^2}$ to characterize the octahedral distortion instead. In our paper, we observe a linear drop in the $c/\sqrt{2}a$ value before the phase transition (consistent with the paper of Kojima *et al.*[5]) and a sudden increase in the value from 1.016 to 1.045 at the orthorhombic phase. Above 5.9 GPa, the value further climbs to 1.048 at 7.6 GPa and then slowly decreases with pressure. One can see from the decrease in the a and b values and the elongation of c, the elevated $c/\sqrt{a^2+b^2}$ value at the orthorhombic phase suggests a higher level of distortion in the AuI_6 octahedra and a relatively closer distance between the Au at (0,0,0) and (1/2,1/2,0) in the ab plane. Below, we further discuss what these observations mean for the two scenarios.

A. Single-valent Au^{II} with space group *Ibmm*

In this structure, as shown in the top panel of Fig. 7, locally equivalent AuI_6 octahedra are elongated and are tilted toward the a axis. The I(2) ions sit at (δx,0,1/4), breaking the fourfold rotational symmetry of the ab plane. If the octahedra are observed from the top of the ab plane, their tilting is around the [110] axis. The AuI_6 octahedra are the same for all Au sites, which is consistent with a single Au^{II} valence. The structural transition at ~5.9 GPa may then be understood as previously suggested by Kojima *et al.*,[5] Kojima,[6] Kojima and Matsushita,[9] and Kitagawa *et al.*:[12] With pressure inducing

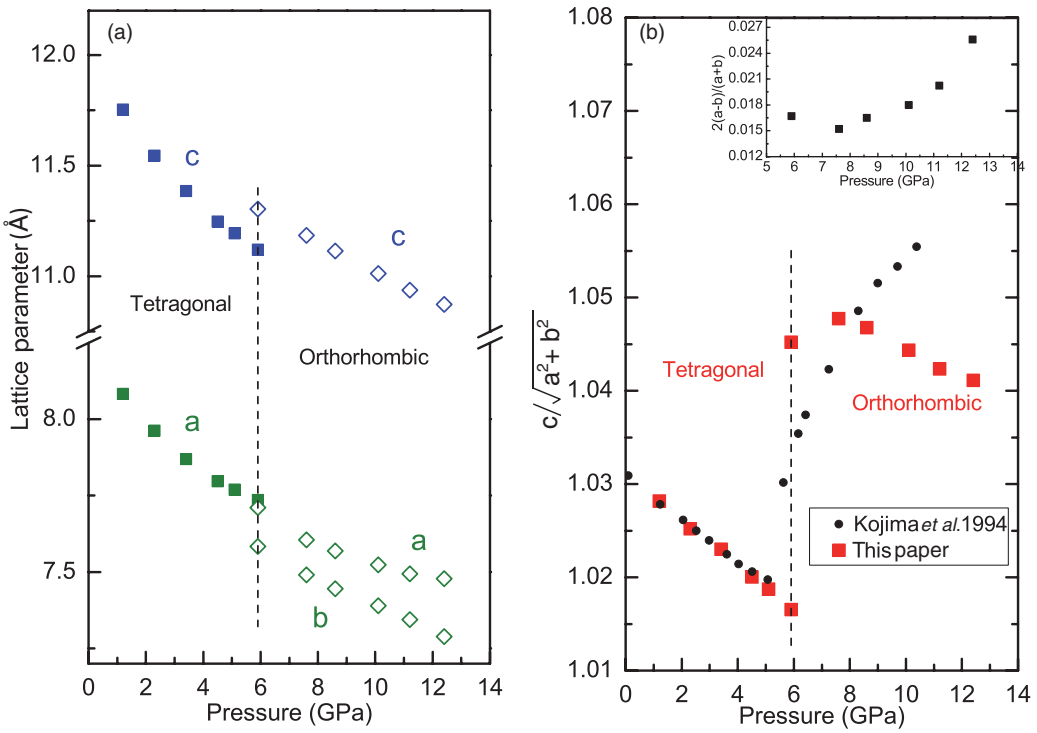

FIG. 6. (Color online) (a) Lattice parameters of $CsAuI_3$ as a function of pressure. Green symbols: a in the tetragonal and a,b in the orthorhombic phases; blue symbols: c. (b) $c/\sqrt{2}a$ and $c/\sqrt{a^2+b^2}$ for tetragonal and orthorhombic phases. Black dots are from a previous paper, which fitted all the phases with the tetragonal space group.[5] Red squares represent this paper. Inset: $2(a-b)/(a+b)$, describing the strain of the orthorhombic cell as a function of pressure. The vertical dashed line marks the onset of the first-order phase transition for increasing pressures.

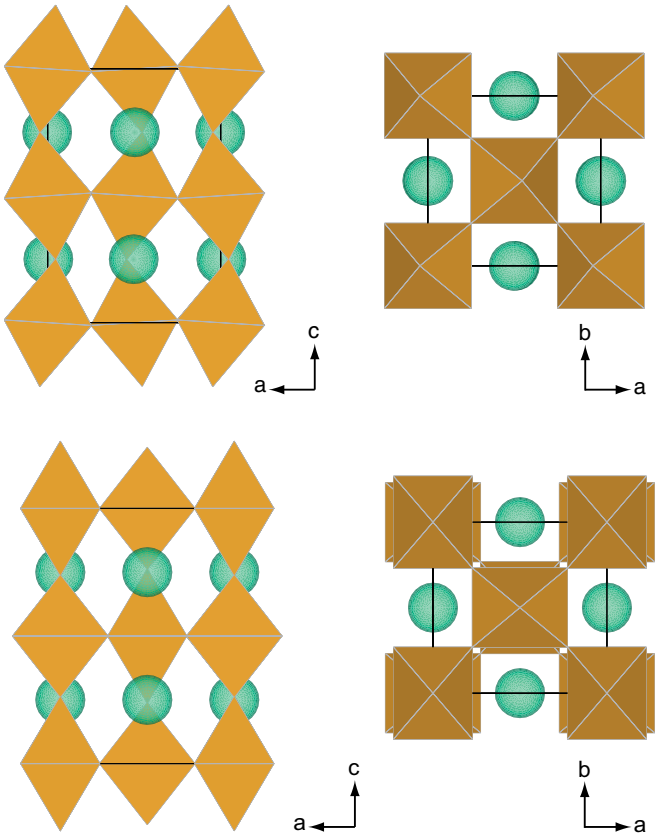

FIG. 7. (Color online) Schematic of the AuI_6 octahedra projection in orthorhombic $CsAuI_3$ at 8.6 GPa. Top panel: the structure with space group *Ibmm*: Locally equivalent octahedra rotate toward the *a* axis and around the [110] plane. Bottom panel: the structure with space group *Immm*: Elongated and compressed octahedra arrange alternatively and do not tilt.

the electron transfer from Au^{I} to Au^{III} (as evidenced by the reduction in the $c/\sqrt{2}a$ ratio) in the lower-pressure tetragonal phase, the MV-SV valence transition is realized at ~5.9 GPa. In the single-valence $Au^{II}I_6$ octahedron, the Au^{II} $5d^9$ electron configuration will have a strong Jahn-Teller effect, causing the sudden increase in the $c/\sqrt{a^2+b^2}$ value. In addition, due to the volume limit imposed by the external pressure, the *c* axis increase alone cannot stabilize the AuI_6 octahedra: They have to tilt to reach a longer Au-I distance in the $5d_{z^2}$ direction.

B. Mixed-valent Au^{I} + Au^{III} with space group *Immm*

In this structure, the AuI_6 octahedra are still distorted but are not tilted. The alternation of elongated and compressed octahedra does not completely vanish and, at least from the perspective of symmetry, still comprises a mixed-valence state of Au^{I} + Au^{III}. This echoes the Mössbauer studies that only see a fully Au^{II} state between 6.6 and 12.5 GPa.[8,9] The new cell geometry (longer *c* axis and closer distances in the *ab* plane) would naturally promote the in-plane Au^{I} ($5d_{x^2-y^2}$) and Au^{I} ($5d_{z^2}$) to Au^{III} ($5d_{x^2-y^2}$) charge transfer, which are the dominant intervalence charge-transfer interactions according to the optical reflectivity measurement and molecular-orbital calculations.[6] Hence, in this scenario, although it is possible that intervalence charge transfer still provides the driving force for the structural transition, nevertheless, the MV-SV transition remains incomplete.

The high-pressure structural transition of $CsAuI_3$, revealed by our paper, differs from that of $CsAuCl_3$ and $CsAuBr_3$. The chloride undergoes a first-order tetragonal $I4/mmm$ $Z = 2$ to a cubic $Pm3m$ $Z = 1$ structural transition at 12.5 GPa, shown by single-crystal x-ray diffraction, and its cubic structure naturally leads to a single Au site with a formal valence Au^{II}.[4] The bromide was shown to undergo a tetragonal $I4/mmm$ $Z = 2$ to a tetragonal $P4/mmm$ $Z = 1$ transition at approximately 9 GPa (Ref. 5) at which pressure the two Au sites also became crystallographically identical. The associated MV-SV transition is consistent with the observation from Raman spectroscopy[7] and the charge-density analysis from synchrotron powder XRD.[21] In the case of $CsAuI_3$, the structural transition, observed at ~5.9 GPa that breaks the tetragonal symmetry, has not been observed in the chloride and bromide.[4–6,9,15,21] If concurrent with the MV-SV transition, it is caused by the Au^{II} $5d^9$ Jahn-Teller effect. If not concurrent with the valence transition, it further promotes the charge transfer between Au^{I} and Au^{III}. Previous Mössbauer studies, showing that a single Au valence is achieved between 6.6 and 12.5 GPa (Refs. 8 and 9), seem to support the notion of an incomplete valence transition at ~5.9 GPa. However, one must note that the measurement was conducted at 4 K at which temperature the first-order transition can be very sluggish. Even in our 300 K measurement, we see a coexistence of the two phases at 5.9 GPa, and it is possible that a larger hysteresis occurs at lower temperatures.

To summarize, we report reversible tetragonal-orthorhombic-amorphous structural transitions in $CsAuI_3$ in a hydrostatic environment up to 21 GPa with critical pressures of 5.5–6 and 12–14 GPa, respectively. Although our results may suggest the MV-SV electronic transition is driving the structure transition (as in the case of the *Ibmm* space group), we cannot rule out the possibility that the valence transition is not completed at the structural transition (if transitioning to a structure of the *Immm* space group), and the charge disproportionation in Au persists into the high-pressure orthorhombic phase. The observation of the orthorhombic phase calls for a more careful study of the structural, electronic, and magnetic properties of $CsAuI_3$ at high pressures to reassess the pressure-induced charge transfer and the MV-SV transition in $CsAuI_3$.

ACKNOWLEDGMENTS

S.W., S.H., and W.L.M. are supported by EFree, an Energy Frontier Research Center funded by the US Department of Energy (DOE), Office of Science, Office of Basic Energy Sciences (BES) under Award No. DE-SG0001057. M.C.S., S.C.R., T.H.G., and I.R.F. are supported by the Airforce Office of Scientific Research (AFOSR) under Grant No. FA9550-09-1-0583. Travel to the experimental facilities was supported through the DOE-NNSA (CDAC). GSECARS is supported through COMPRES under NSF Cooperative Agreement No. EAR 10-43050. ALS is supported by the DOE-BES under Contract No. DE-AC02-05CH11231.

[1]I. Jarrige, H. Ishii, Y. Q. Cai, J.-P. Rueff, C. Bonnelle, T. Matsumura, and S. R. Shieh, Phys. Rev. B **72**, 075122 (2005).
[2]H. Kitagawa, N. Kojima, N. Matsushita, T. Ban, and I. Tsujikawa, J. Chem. Soc., Dalton Trans. 3115 (1991).
[3]H. Kitagawa, N. Kojima, and T. Nakajima, J. Chem. Soc., Dalton Trans. 3121 (1991).
[4]N. Matsushita, H. Ahsbahs, S. S. Hafner, and N. Kojima, J. Solid State Chem. **180**, 1353 (2007).
[5]N. Kojima, M. Hasegawa, H. Kitagawa, T. Tikegawa, and O. Shimomura, J. Am. Chem. Soc. **116**, 11368 (1994).
[6]N. Kojima, Bull. Chem. Soc. Jpn. **73**, 1445 (2000).
[7]X. J. Liu, K. Matsuda, Y. Moritomo, A. Nakamura, and N. Kojima, Phys. Rev. B **59**, 7925 (1999).
[8]S. S. Hafner, N. Kojima, J. Stanek, and L. Zhang, Phys. Lett. A **192**, 385 (1994).
[9]N. Kojima and N. Matsushita, Coord. Chem. Rev. **198**, 251 (2000).
[10]N. Elliott and L. Pauling, J. Am. Chem. Soc. **60**, 1846 (1938).
[11]N. Matsushita, H. Kitagawa, and N. Kojima, Acta Crystallographica Section C **53**, 663 (1997).
[12]H. Kitagawa, H. Sato, N. Kojima, T. Kikegawa, P. Factory, and O. Shimomura, Solid State Commun. **78**, 989 (1991).
[13]A. F. Kusmartseva, M. Yang, A. M. Arevalo-Lopez, K. V. Kamenev, and J. P. Attfield, Chem. Commun. (Cambridge) **46**, 6681 (2010).
[14]M. Trigo, J. Chen, M. P. Jiang, W. L. Mao, S. C. Riggs, M. C. Shapiro, I. R. Fisher, and D. A. Reis, Phys. Rev. B **85**, 081102(R) (2012).
[15]W. Denner, H. Schulz, and H. d'Amour, Acta Crystallographica Section A **35**, 360 (1979).
[16]S. Riggs, M. Shapiro, F. Corredor, T. Geballe, I. R. Fisher, G. T. Mccandless, and J. Y. Chan, J. Cryst. Growth **355**, 13 (2012).
[17]H. K. Mao, J. Xu, and P. M. Bell, J. Geophys. Res. **91**, 4673 (1986).
[18]A. P. Hammersley, S. O. Svensson, M. Hanfland, A. N. Fitch, and D. Hausermann, High Press. Res. **14**, 235 (1996).
[19]B. H. Toby, J. Appl. Crystallogr. **34**, 210 (2001).
[20]E. Climent-Pascual, N. Ni, S. Jia, Q. Huang, and R. Cava, Phys. Rev. B **83**, 174512 (2011).
[21]M. Sakata, T. Itsubo, E. Nishibori, Y. Moritomo, N. Kojima, Y. Ohishi, and M. Takata, J. Phys. Chem. Solids **65**, 1973 (2004).